Tensile failure prediction of U-notched plates under moderate-scale and large-scale yielding regimes

A.R. Torabi [a,*], F. Berto [b], S.M.J. Razavi [b]

[a] *Fracture Research Laboratory, Faculty of New Sciences & Technologies, University of Tehran, P.O. Box 14395-1561, Tehran, Iran.*

[b] *NTNU, Department of Mechanical and Industrial Engineering, Richard Birkelands vei 2b, 7491 Trondheim, Norway.*

Abstract

The main goal of the present research is to check if the recently published experimental results on tensile load-carrying capacity (LCC) of ductile U-notched Al 7075-T6 and Al 6061-T6 plates could successfully be predicted by means of combining the Equivalent Material Concept (EMC) with the Averaged Strain Energy Density (ASED) criterion, which is fundamentally a brittle fracture criterion. By using the two main material properties, namely the fracture toughness and the tensile strength of the equivalent material, which is extracted from the EMC, the maximum load that each notched plate could sustain is predicted by means of the combined EMC-ASED criterion. It is revealed that the EMC-ASED criterion is capable of predicting well the LCC of both aluminum plates, independent of the level of ductility of materials and the size of plastic region around the notch at crack initiation instance.

Keywords: Averaged Strain Energy Density (ASED); Ductile failure; Equivalent Material Concept (EMC); Large-scale yielding (LSY); Moderate-scale yielding (MSY); U-notch.

* Corresponding author: A.R. Torabi, Tel.: +98 21-61 118 572, Fax: +98 21-88 497324, E-mail: a_torabi@ut.ac.ir (A.R. Torabi)

1. Introduction

Due to some specific design requirements such as connecting two or more parts together, transmitting load from one component to another, repairing cracked or damaged structures etc., most of engineering components and structures contain notches of different shapes e.g. V-, U-, O- and key-hole notches. Beside their usefulness, notches are prone to crack initiation due to the stress concentration at their neighborhood. Such crack(s) may propagate and lead to final fracture of the notched component. Therefore, it is generally attempted in design of notched components and structures to prevent or delay the crack initiation from the notch border [1-5]. For this purpose, appropriate failure criteria are essentially needed to accurately predict such a crack initiation.

From the viewpoint of solid mechanics, engineering materials are located in three general categories of brittle, quasi-brittle and ductile materials. The main characteristics of brittle and quasi-brittle materials are their relatively low strain to failure and sudden (or rapid) fracture, while in most of ductile materials, the strain to failure is considerable and the fracture phenomenon is progressive and stable. Because of two main reasons, researchers' time has been mostly spent on brittle fracture of notched members and hence, the number of research works on ductile failure is relatively limited. The first reason is definitively the simplicity of brittle materials failure analysis which is normally carried out by assuming the linear elastic material behavior. The second one and really more important one is, however, the catastrophic nature of brittle fracture, which may lead to heavy damages to engineering structures. Although failure analysis of notched ductile components exhibiting elastic-plastic behavior (particularly, ductile metallic components) is much more complex than that of notched brittle components, it is also necessary to be performed due to the widespread applications of ductile materials in engineering

structures, e.g. aluminum alloys in aerial vehicles etc. Recently, some research works have been performed on ductile failure of notches under various loading conditions [6-20].

The first research specifically focused on ductile failure of notched metallic components was performed by Susmel and Taylor [6]. They made use of the well-known Theory of Critical Distances (TCD), which is fundamentally a theory for predicting fracture in brittle materials exhibiting linear-elastic behavior, for estimating the load-carrying capacity (LCC) of V-, U- and O-notched ductile steel plates under pure mode I loading, encountering large plasticity at the notch vicinity at the onset of crack initiation from the notch tip [6]. While agreement with the experimental results was surprisingly good, it could not strongly be justified that how the linear-elastic TCD could predict the failure results in the presence of the large-scale yielding (LSY) regime [6]. In order to make an appropriate justification to such an agreement, Torabi [7] proposed the Equivalent Material Concept (EMC) by which ductile material showing elastic-plastic behavior and having valid *K*-based fracture toughness (K_{Ic} or K_c) is equated with a virtual brittle material exhibiting perfectly linear-elastic behavior. Thanks to EMC, the tensile LCCs of notched ductile steel plates and bolts were successfully predicted by using only the linear-elastic analyses [7-10].

To check whether EMC is capable of being combined with brittle fracture criteria in the context of the linear-elastic notch fracture mechanics (LENFM) for predicting failure in engineering components made of ductile materials other than the steel materials reported in Refs. [6, 10], some new ductile failure analyses have been recently carried out by Torabi and co-researchers [11-17] on notched aluminum plates under different in-plane loading conditions. They have published seven papers on this subject; three on pure mode I loading [11, 13, 15] and four on mixed mode I/II loading [12, 14, 16, 17]. It can be seen in Refs. [11-17] that EMC has been

linked to the two well-known stress-based brittle fracture criteria, namely the maximum tangential stress (MTS) and mean stress (MS) criteria, making it possible to wave the considerable plastic region at the notch neighborhood and predict well the LCCs of the U- and V-notched Al 7075-T6 and Al 6061-T6 plates using the linear- elastic analyses. It has been reported in Refs. [11-17] that the notched Al 7075-T6 and Al 6061-T6 plates fail by moderate-scale yielding (MSY) and large-scale yielding (LSY) regimes, respectively under pure mode I loading, while all of the notched aluminum specimens fail by large-scale yielding (LSY) regime under mixed mode I/II loading conditions.

More recently, Torabi and co-researchers [18-20] have linked EMC to an energy-based brittle fracture criterion, namely the averaged strain energy density (ASED) criterion, in order to predict the experimentally obtained LCCs of the aluminum plates reported in Refs. [11, 16, 17] without performing elastic-plastic analyses. Very good agreements have been found to exist between the theoretical results of the EMC-ASED criterion and the experimental results.

To check whether the combined EMC-ASED criterion works well on tensile failure prediction of U-notches in both MSY and LSY regimes, it is attempted in the present study to predict the experimentally obtained tensile LCCs of the U-notched Al 7075-T6 and Al 6061-T6 plates reported in Ref. [13] by means of the EMC-ASED criterion. Good agreements are revealed to exist between the experimental results and theoretical predictions for both of the aluminum plates. Since Al 7075-T6 and Al 6061-T6 plates have failed by the MSY and LSY regimes, respectively [13], such good agreements suggest that the validity of EMC-ASED criterion does not considerably depend on the size of the plastic zone around the notch border at failure.

2. Experimental results on MSY and LSY failure of U-notches

Recently, a research paper has been published in the open literature providing some experimental results on tensile failure of U-notches encountering MSY and LSY regimes [13]. The test specimen has been simply a rectangular plate of finite thickness containing a central bean-shaped slit with two U-shaped ends horizontally located (see Fig. 1).

Fig. 1. Scheme of the test specimen with the geometric parameters included [13].

To provide moderate and large amounts of plasticity around the notch at crack initiation instance, Torabi et al. [13] have intentionally selected Al 7075-T6 and Al 6061-T6 materials, which both are ductile materials with significantly different values of the tensile strain at the ultimate point. Table 1 presents some of the mechanical properties of the Al 7075-T6 and Al 6061-T6 alloys [13]. Fig. 2 also represents the standard tensile stress-strain curves for both materials in the engineering and true formats [13]. Note that thickness for the Al 7075-T6 and Al 6061-T6 notched plates has been equal to 2 mm and 4 mm, respectively; both are relatively thin, providing considerable plasticity around the notch at failure as a result of nearly the plane-stress conditions. This is the main reason for reporting in Table 1 the values of the fracture toughness (K_c) instead of those of the plane-strain fracture toughness (K_{Ic}).

Table 1. Some of the mechanical properties of the Al 7075-T6 and Al 6061-T6 alloys [13].

Fig. 2. Standard tensile stress-strain curves for the Al 7075-T6 and Al 6061-T6 alloys in the engineering and true formats [13].

In Fig. 1, the parameters ρ, 2a, L, W, and P denote the notch radius, twice the notch length (i.e. the slit length), the specimen length, the specimen width, and the applied tensile load, respectively. The values of the geometric parameters included in the experiments have been equal to: ρ = 0.5, 1, and 2 mm; 2a = 25 mm; L = 160 mm; and W = 50 mm. By repeating the test for each notch radius three times, 9 tests have been carried out for each material; all in all, 18 tensile failure tests have been performed and reported in Ref. [13]. A high-precision two-dimensional (2D) water jet cutting machine has been utilized to fabricate the specimens [13]. Moreover, the tensile fracture experiments have been carried out under displacement-control conditions at a strain rate of about 1.5×10^{-3} m/min providing monotonic loading conditions.

Table 2 summarizes the experimentally obtained LCCs of the U-notched Al 7075-T6 and Al 6061-T6 plates for different notch radii [13]. The parameters P_i (i=1, 2, 3) and P_{av} denote the LCC in the three repeated tests and the average of the three LCCs, respectively.

Table 2. Experimentally obtained tensile LCCs of the U-notched Al 7075-T6 and Al 6061-T6 plates for various notch radii [13].

Some of the U-notched Al 7075-T6 and Al 6061-T6 plates are depicted in Fig. 3 after tensile rupture.

Fig. 3. The U-notched Al 7075-T6 and Al 6061-T6 plates after fracture; (a), (c): Al 7075-T6 and (b), (d): Al 6061-T6.

In Figs. 3(a) and (b), it is seen by the naked eye that both specimens experience considerable plastic deformations before rupture; indeed, the Al 6061-T6 specimen exhibits much more clear deformations. It is evident that the total plastic region at the specimen ligament is divided into two portions. The first portion forms before the crack initiation from the notch tip and the second portion forms during the crack growth phase (till final rupture). Since the LCC of the notched aluminum plates, which is obtained at the onset of crack initiation, is studied in the present research, determining the type of failure regime in the plates should be performed based on the plastic zone size at the crack initiation instance. It has been reported in Ref. [13] that both the experimental observations and the elastic-plastic finite element (FE) analyses demonstrated that the U-notched Al 7075-T6 and Al 6061-T6 plates failed by the MSY and LSY regimes, respectively. Figs. 3(c) and (d) represent the fracture surfaces of the two U-notched plates in a close view. The inclined fracture surfaces clearly suggest the ductile rupture of the specimens, since ductile rupture in metallic materials takes place usually in the plane of maximum shear stress. Based on the fact that the size of the plastic zone around the notch at failure has been small in none of the tested aluminum plates [13], it is not fundamentally permitted to use brittle fracture criteria; e.g. the ASED criterion etc., that most of them have been developed considering the linear-elastic material behavior, for predicting the experimentally obtained LCCs. Thus, the EMC is briefly described in the next section and linked to the ASED criterion with the aim to take a permission to use the linear-elastic-based ASED criterion for predicting the MSY and LSY failure of the U-notched aluminum plates.

3. The Equivalent Material Concept

Torabi [7] suggested the Equivalent Material Concept (EMC) with the aim to avoid utilizing time-consuming and complex ductile failure criteria for predicting the LCC of notched ductile components. According to EMC, a ductile material with valid *K*-based fracture toughness (i.e. K_{Ic} or K_c) and elastic-plastic behavior is equated with a virtual brittle material with an ideal linear elastic behavior till final fracture. It is assumed that the virtual brittle material has the same Young's modulus, Poisson's ratio and *K*-based fracture toughness (K_{Ic} or K_c) as the real ductile material, but it has different tensile strength. Assuming that both the materials absorb the same amount of tensile strain energy density (SED) for the crack initiation to take place (i.e. the area under the standard tensile stress-strain curve from the start point till the ultimate point), the tensile strength of the equivalent material could be calculated. The tensile strength calculated for the equivalent material and the fracture toughness K_{Ic} or K_c can simultaneously be used in various brittle fracture criteria, such as the ASED, for predicting the LCC of notched ductile components by using the linear elastic analysis. A full description of EMC can be found in some recent references, e.g. Refs. [11-20]. However, for the sake of brevity, it is preferred herein to present directly the formulation of the tensile strength of the equivalent material. Considering the power-law relationship between the stress and the plastic strain for the ductile material, a closed-form expression has been achieved for the tensile strength of the equivalent material as a function of some tensile properties of the ductile material as follows [13]:

$$\sigma_f^* = \sqrt{{\sigma_Y}^2 + \frac{2EK}{n+1}\left[{\varepsilon_{u,true}}^{n+1} - (0.002)^{n+1}\right]} \tag{1}$$

In Eq. 1, the parameters σ_f^*, σ_Y, E, K, n, and $\varepsilon_{u,\text{true}}$ denote the tensile strength of the equivalent material, yield strength of the ductile material, Young's modulus, strain-hardening coefficient, strain-hardening exponent, and the true plastic strain at the ultimate point, respectively. The value of $\varepsilon_{u,\text{true}}$ can simply be computed by using the equation $\varepsilon_{u,true} = \ln(1+\varepsilon_u)$, where the parameter ε_u is the engineering plastic strain at the ultimate point.

The values of σ_f^* for the Al 7075-T6 and Al 6061-T6 materials can be computed by substituting the values of the tensile properties presented in Table 1 into Eq. 1 to be equal to about 1845 MPa and 1066 MPa, respectively. Such values can now be utilized together with the K_c values presented in Table 1 inside the ASED criterion for predicting the experimentally obtained LCCs of the U-notched aluminum plates summarized in Table 2. In forthcoming sections, the ASED criterion is briefly described and the experimental LCCs of the aluminum plates are theoretically predicted using the EMC-ASED criterion.

4. The Averaged Strain Energy Density criterion for failure load prediction

Various failure criteria have been proposed in the literature in order to estimate the LCC of structural components made of various materials with different geometries. Among the available failure criteria, a strain energy density based criterion has been first proposed by Lazzarin and Zambardi [22]. According to the averaged strain energy density (ASED) criterion, brittle fracture occurs when the mean value of SED over material dependent control volume reaches a critical value of W_c which depends on the material. The critical SED value is not dependent on the notch geometry. Considering a linear elastic behavior for the material, the control volume depends on

the ultimate tensile strength and the fracture toughness K_{Ic}. The ASED was first developed for V-notched specimens under pure mode I and in-plane mixed mode loading conditions. Later on it was used for LCC prediction of various geometries of notches and various brittle and quasi-brittle materials [23-28].

For a specific case of a sharp crack, the control volume is a circle of radius R_c centered at the crack tip (Fig. 4b). Considering plane-strain condition, the radius of control volume R_c, can be calculated using [22]

$$R_c = \frac{(1+\nu)(5-8\nu)}{4\pi}\left(\frac{K_{Ic}}{\sigma_u}\right)^2 \tag{3}$$

where K_{Ic}, ν and σ_u are the mode I fracture toughness, the Poisson's ratio and the ultimate tensile strength of material. On the other hand, for a U-notch under mode I loading, the volume becomes a crescent shape shown in Fig. 4b, where R_c is the depth measured along the notch bisector line. The external radius of the crescent shape volume is equal to $R_c+.\rho/2$.

Fig. 4. Control volume (area) for sharp crack (a) and U-notch (c) under mode I loading.

5. Application of combined EMC-ASED criterion for LCC prediction

The ASED criterion was used for the LCC prediction of ductile materials equated to linear elastic material. Using the equivalent ultimate tensile strength and elastic modulus, one can calculate the critical strain energy density, $W_{c,EMC}$ using the expression below:

$$W_{c,EMC} = \frac{\sigma_f^{*2}}{2E} \quad (4)$$

The critical strain energy density results to be equal to 23.97 MJ/m^3 and 8.48 MJ/m^3 for Al 7075-T6 and Al 6061-T6 materials, respectively. By using Eq. (3) and considering $\sigma_u = \sigma_f^*$, the control radius R_c is found as 0.183 mm and 0.317 mm for Al 7075-T6 and Al 6061-T6 materials, respectively. The average value of SED inside the control volume ($\overline{W}$) is calculated numerically by using finite element analysis. Considering different notch root radii, the geometry of control volume is different for the analyzed models. According to the procedure described in the previous section, the control volume is centered along the bisector line of the notch. Eight-node 2D finite elements under plane-strain conditions are used for meshing the models. A typical view of the mesh and the SED contour lines are illustrated in Fig. 5.

Fig. 5: Typical mesh used in the FE model and strain energy density contour lines in the control volume for the Al 6061-T6 model with notch root radius of ρ=1 mm.

6. Results and discussion

Different notch radii of ρ = 1, 2, 4 mm are analyzed by means of the ASED approach for two different aluminum alloys of Al 7075-T6 and Al 6061-T6. The results of the experimental, numerical and theoretical analyses for U-notched specimens are presented in Table 3. In particular, Table 3 reports the experimental loads to failure (P) for all notch radii ρ compared with the theoretical values (P_{ASED}) based on the ASED evaluation. Considering constant values

of the critical strain energy density, $W_{c,EMC}$, equal to 23.97 MJ/m^3 and 8.48 for Al 7075-T6 and Al 6061-T6 materials gives the theoretical load of P_{ASED}.

Table 3. Critical loads predicted for U-notched specimens by means of ASED criterion in combination with EMC.

The relative deviations between the experimental failure loads and the theoretical predictions obtained by means of ASED criterion are reported in the last columns of the table to show the accuracy of the combined ASED-EMC approach. The ratio of the experimental load and the theoretical one is defined as Δ. Considering the results available in Table 3, it is obvious that the majority of LCC predictions are well inside the scatter band ranging between ± 20% with considerable number of the results falling inside the scatter ranging between ± 10%.

Fig. 6 illustrates a comprehensive synthesis expressed in terms of the square root of the mean value of the strain energy normalized by the critical energy of the material, $W_{c,EMC}$, as a function of the notch root radius ρ. The parameter plotted in the figure is proportional to the failure load. According to the data available in the presented synthesis, it is verified that the chosen control volume is suitable to characterize the failure of the ductile materials containing U-notches. Comparing the scatter of assessed experimental results in this paper with the recent database in terms of ASED reported in a review of the approach and dealing with brittle and quasi-brittle failure [29] shows a very good agreement. According to the importance of the mechanical behaviour of notched components under fatigue and creep loading conditions, the same

methodology can be extended to evaluate the failure of notched components under fatigue and creep loading conditions [30-37].

Fig. 6. Synthesis of fracture data in terms of normalized ASED; (a) Al 7075-T6, (b) Al 6061-T6.

7. Conclusions

Ductile failure of the U-notched aluminum specimens was investigated by equating the real ductile material with a brittle material having a virtual ultimate strength. Various notch radii were considered for the specimens made of Al 7075-T6 and Al 6061-T6. Fracture tests were undertaken on rectangular plate of finite thickness containing a central bean-shaped slit with two U-shaped ends horizontally located under mode I loading. According to the experimental results, the U-notched Al 7075-T6 and Al 6061-T6 plates failed by the MSY and LSY regimes, respectively. The Equivalent Material Concept was used to have equivalent brittle materials to be capable for application of the Averaged Strain Energy Density over a material-dependent control volume. Using this combined approach, without requiring time-consuming and complex elastic-plastic finite element analyses, the load-carrying capacity of the U-notched Al 7075-T6 and Al 6061-T6 plates were successfully predicted.

References

[1] S.M.J. Razavi, M.R. Ayatollahi, C. Sommitsch, C. Moser, Retardation of fatigue crack growth in high strength steel S690 using a modified stop-hole technique, Eng. Fract. Mech. 169 (2017) 226–237.

[2] M.R. Ayatollahi, S.M.J. Razavi, C. Sommitsch, C. Moser, Fatigue life extension by crack repair using double stop-hole technique, Mater. Sci. Forum 879 (2017) 3-8.

[3] M. R. Ayatollahi, S.M.J. Razavi, M.Y. Yahya, Mixed mode fatigue crack initiation and growth in a CT specimen repaired by stop hole technique, Eng. Fract. Mech. 145 (2015) 115-127.

[4] M.R. Ayatollahi, S.M.J. Razavi, H.R. Chamani, A numerical study on the effect of symmetric crack flank holes on fatigue life extension of a SENT specimen. Fatigue Fract. Eng. Mater. Struct. 37(10) (2014) 1153-1164.

[5] M.R. Ayatollahi, S.M.J. Razavi, H.R. Chamani, Fatigue Life Extension by Crack Repair Using Stop-hole Technique under Pure Mode-I and Pure mode-II Loading Conditions, Procedia Eng. 74 (2014) 18–21.

[6] L. Susmel, D. Taylor, On the use of the Theory of Critical Distances to predict static failures in ductile metallic materials containing different geometrical features, Eng. Fract. Mech. 75 (2008) 4410-4421.

[7] A.R. Torabi, Estimation of tensile load-bearing capacity of ductile metallic materials weakened by a V-notch: The equivalent material concept, Mater. Sci. Eng. A. 536 (2012) 249–255.

[8] A.R. Torabi, Ultimate bending strength evaluation of U-notched ductile steel samples under large-scale yielding conditions, Int. J. Fract. 180 (2013) 261–268.

[9] A.R. Torabi, The Equivalent Material Concept: Application to failure of O-notches, Eng.

Solid Mech. 1 (2013) 129–140.

[10] A.R. Torabi, On the use of the Equivalent Material Concept to predict tensile load-bearing capacity of ductile steel bolts containing V-shaped threads, Eng. Fract. Mech. 97 (2013) 136–147.

[11] A. Torabi, M. Alaei, Application of the equivalent material concept to ductile failure prediction of blunt V-notches encountering moderate-scale yielding, Int. J. Damage Mech. 25(6) (2016) 853-877.

[12] A.R. Torabi, M. Alaei, Mixed-mode ductile failure analysis of V-notched Al 7075-T6 thin sheets, Eng. Fract. Mech. 150 (2015) 70–95.

[13] A.R. Torabi, R. Habibi, B. Mohammad Hosseini, On the ability of the Equivalent Material Concept in predicting ductile failure of U-notches under moderate- and large-scale yielding conditions, Phys. Mesomech. 18 (2015) 337–347.

[14] A.R. Torabi, R. Habibi, Investigation of ductile rupture in U-notched Al 6061-T6 plates under mixed mode loading, Fatigue Fract. Eng. Mater. Struct. 39 (2016) 551-565.

[15] A.R. Torabi, M. Keshavarzian, Tensile crack initiation from a blunt V-notch border in ductile plates in the presence of large plasticity at the notch vicinity, Int. J. Terraspace Sci. Eng. 8(1) (2016) 93-101.

[16] A.R. Torabi, M. Keshavarzian, Evaluation of the load-carrying capacity of notched ductile plates under mixed mode loading, Theor. Appl. Fract. Mech. 85 (2016) 375-386.

[17] A.R. Torabi, B. Mohammad Hosseini, Large plasticity induced crack initiation from U-notches in thin aluminum sheets under mixed mode loading, Eng. Solid Mech. 5(1) (2017)

39-60.

[18] A.R. Torabi, F. Berto, A. Campagnolo, Elastic-plastic fracture analysis of notched Al 7075-T6 plates by means of the local energy combined with the equivalent material concept, Phys. Mesomech. 19 (2016) 204–214.

[19] A.R. Torabi, A. Campagnolo, F. Berto, Mixed mode I/II crack initiation from U-notches in Al 7075-T6 thin plates by large-scale yielding regime, Theor. Appl. Fract. Mech. 86 (2016) 284-291.

[20] A.R. Torabi, A. Campagnolo, F. Berto, A successful combination of the equivalent material concept and the averaged strain energy density criterion for predicting crack initiation from blunt V-notches in ductile aluminum plates under mixed mode loading, Phys. Mesomech. 19(4) (2016) 382-391.

[21] A. Torabi, F. Berto, S.M.J. Razavi, Ductile failure prediction of thin notched aluminum plates subjected to combined tension-shear loading, Theor. Appl. Fract. Mech. (in press) (DOI: 10.1016/j.tafmec.2017.05.003).

[22] P. Lazzarin, R. Zambardi, A finite-volume-energy based approach to predict the static and fatigue behavior of components with sharp V-shaped notches, Int. J. Fract. 112 (2001) 275–298.

[23] F. Berto, P. Lazzarin, A review of the volume-based strain energy density approach applied to V-notches and welded structures, Theor. Appl. Fract. Mech. 52 (2009) 183–194.

[24] P. Gallo, F. Berto, Advanced Materials for Applications at High Temperature: Fatigue Assessment by Means of Local Strain Energy Density, Adv. Eng. Mater. (in Press) DOI:10.1002/adem.201500547

[25] P. Gallo, F. Berto, High temperature fatigue tests and crack growth in 40CrMoV13.9 notched components, Frattura ed Integrita Strutturale 9 (2015) 180-189.

[26] P. Gallo, F. Berto, G. Glinka, Analysis of creep stresses and strains around sharp and blunt V-notches, Theor. Appl. Fract. Mech. (in Press) DOI: 10.1016/j.tafmec.2016.06.003

[27] P. Gallo, T. Sumigawa, T. Kitamura, F. Berto, Analysis of creep stresses and strains around sharp and blunt V-notches, Fatigue Fract. Eng. Mater. Struct. (in Press) DOI: 10.1111/ffe.12468.

[28] P. Gallo, F. Berto, G. Glinka, Generalized approach to estimation of strains and stresses at blunt V-notches under non-localized creep, Fatigue Fract. Eng. Mater. Struct. 39(3) (2016) 292-306.

[29] F. Berto, P. Lazzarin, Recent developments in brittle and quasi-brittle failure assessment of engineering materials by means of local approaches, Mater. Sci. Eng. Reports 75 (2014) 1–48.

[30] K.K. Tang, S.H. Li, Interactive creep–fatigue crack growth of 2024-T3 Al sheets: selective transitional functions, Fatigue Fract. Eng. Mater. Struct. 38 (2015) 597-609.

[31] K.K. Tang, H. Wu, F. Berto, Fatigue data interpretation of 7075-T6 Al sheets by energy density factor in a dual scale model, Theor. Appl. Fract. Mech. 79 (2015) 98-104.

[32] K.K. Tang, F. Berto, H. Wu, Fatigue crack growth in the micro to large scale of 7075-T6 Al sheets at different R ratios. Theor. Appl. Fract. Mech. 83 (2016) 93-104.

[33] Y. Liu, S. Mahadevan, Fatigue limit prediction of notched components using short crack growth theory and an asymptotic interpolation method, Eng. Fract. Mech. 76(15) (2009) 2317-2331.

[34] K. Tanaka, Small fatigue crack propagation in notched components under combined torsional and axial loading, Procedia Eng. 2(1) (2010) 27-46.

[35] D. Barbera, H. Chen, Y. Liu, Advances on creep–fatigue damage assessment in notched components, Fatigue Fract. Eng. Mater. Struct. (in press) (DOI: 10.1111/ffe.12603)

[36] H. Chen, A.R.S. Ponter, Linear matching method on the evaluation of plastic and creep behaviours for bodies subjected to cyclic thermal and mechanical loading, Int. J. Numer. Meth. Eng. 68(1) (2006) 13-32.

[37] M.S. Habibullah, A.R.S. Ponter, A crack tip field estimation technique for the high-temperature cyclic loading of structures, Fatigue Fract. Eng. Mater. Struct. 29(5) (2006) 373-387.

Figure captions

Fig. 1. Scheme of the test specimen with the geometric parameters included [8].

Fig. 2. Standard tensile stress-strain curves for the Al 7075-T6 and Al 6061-T6 alloys in the engineering and true formats [8].

Fig. 3. The U-notched Al 7075-T6 and Al 6061-T6 plates after fracture; (a), (c): Al 7075-T6 and (b), (d): Al 6061-T6.

Fig. 4. Control volume (area) for sharp crack (a) and U-notch (c) under mode I loading [16].

Fig. 5: Typical mesh used in the FE model and strain energy density contour lines in the control volume for the Al 6061-T6 model with notch root radius of ρ=1 mm.

Fig. 6. Synthesis of fracture data in terms of normalized ASED; (a) Al 7075-T6, (b) Al 6061-T6.

Table captions

Table 1. Some of the mechanical properties of the Al 7075-T6 and Al 6061-T6 alloys [8].

Table 2. Experimentally obtained tensile LCCs of the U-notched Al 7075-T6 and Al 6061-T6 plates for various notch radii [8].

Table 3. Critical loads predicted for U-notched specimens by means of ASED criterion in combination with EMC.

Table 1. Some of the mechanical properties of the Al 7075-T6 and Al 6061-T6 alloys [8].

Material Property	Value for Al 7075-T6	Value for Al 6061-T6
Young's modulus, E (GPa)	71	67
Poisson's ratio	0.33	0.33
Tensile yield strength (MPa)	521	276
Ultimate tensile strength (MPa)	583	292
Elongation at break (%)	5.8	11
Engineering strain at maximum load	0.047	0.034
True fracture stress (MPa)	610	299
Fracture toughness, K_c (MPa$\sqrt{\text{m}}$)	50	38
Strain-hardening coefficient, (MPa)	698	314
Strain-hardening exponent	0.046	0.021

Table 2. Experimentally obtained tensile LCCs of the U-notched Al 7075-T6 and Al 6061-T6 plates for various notch radii [8].

ρ (mm)	P_1 (N)	P_2 (N)	P_3 (N)	$P_{av.}$ (N)
Al 7075-T6				
0.5	25424	24982	25700	25369
1	27668	27083	28043	27598
2	30236	30475	30041	30250
Al 6061-T6				
0.5	29459	29191	29338	29329
1	31181	30283	31001	30822
2	33068	33300	33366	33245

Table 3. Critical loads predicted for U-notched specimens by means of ASED criterion in combination with EMC.

ρ (mm)	P_1 (N)	P_2 (N)	P_3 (N)	$P_{av.}$ (N)	P_{ASED} (N)	Δ_1	Δ_2	Δ_3
Al 7075-T6								
0.5	25424	24982	25700	25369	21557	1.18	1.16	1.19
1	27668	27083	28043	27598	24321	1.14	1.11	1.15
2	30236	30475	30041	30250	29169	1.04	1.04	1.03
Al 6061-T6								
0.5	29459	29191	29338	29329	31178	0.94	0.94	0.94
1	31181	30283	31001	30822	32013	0.97	0.95	0.97
2	33068	33300	33366	33245	35895	0.92	0.93	0.93

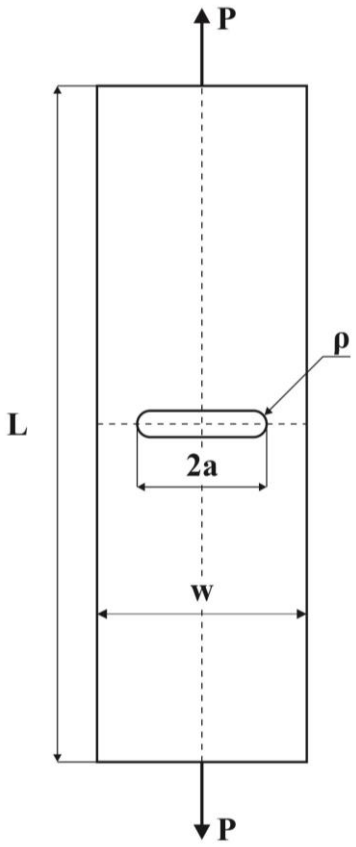

Fig. 1. Scheme of the test specimen with the geometric parameters included [8].

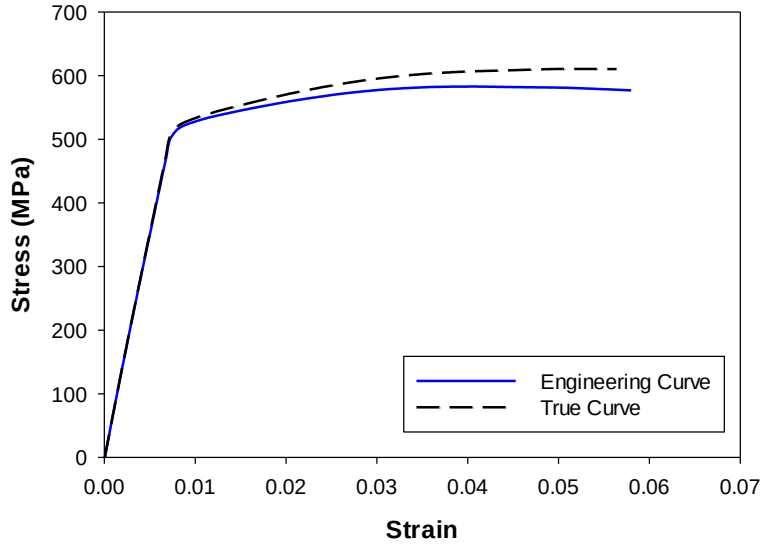

(a) Al 7075-T6

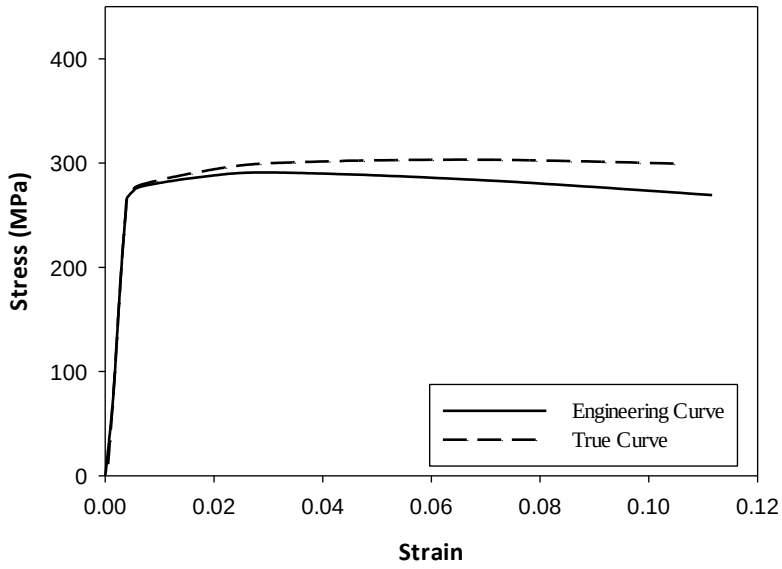

(b) Al 6061-T6

Fig. 2. Standard tensile stress-strain curves for the Al 7075-T6 and Al 6061-T6 alloys in the engineering and true formats [8].

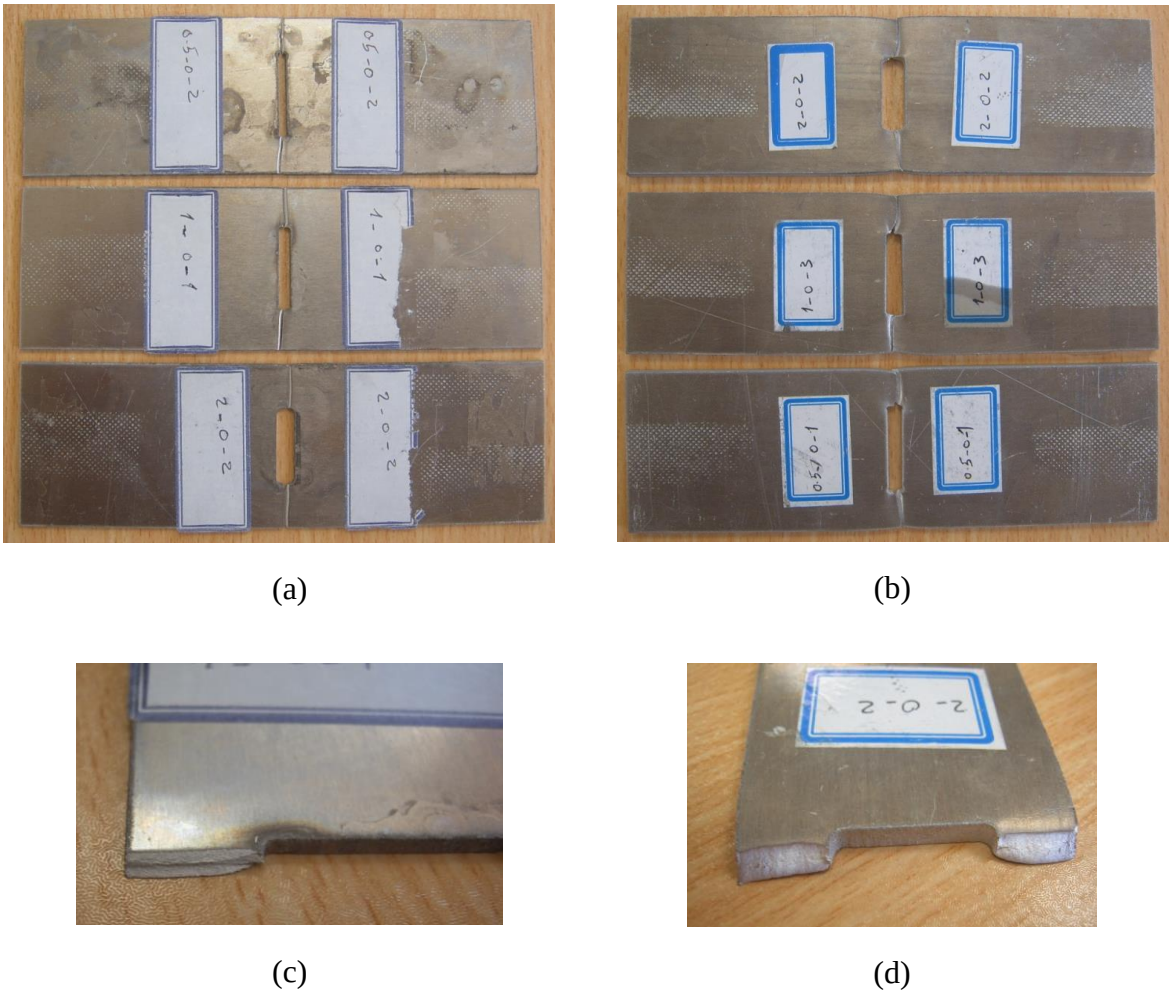

(a) (b)

(c) (d)

Fig. 3. The U-notched Al 7075-T6 and Al 6061-T6 plates after fracture; (a), (c): Al 7075-T6 and (b), (d): Al 6061-T6.

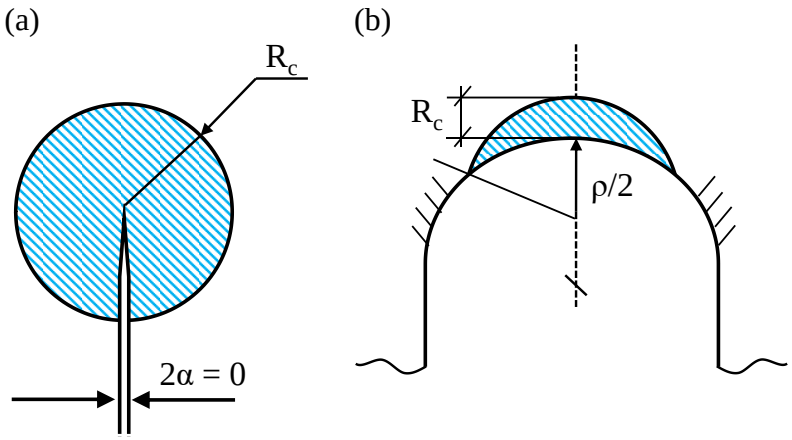

Fig. 4. Control volume (area) for sharp crack (a) and U-notch (c) under mode I loading [16].

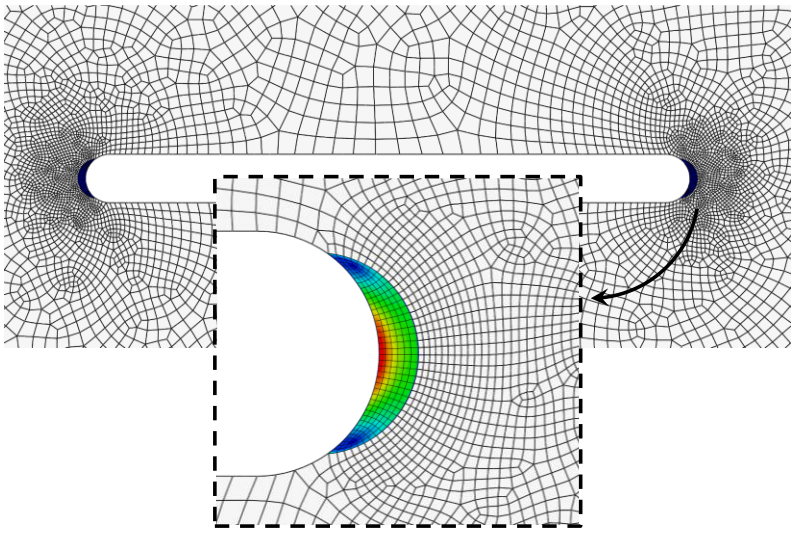

Fig. 5: Typical mesh used in the FE model and strain energy density contour lines in the control volume for the Al 6061-T6 model with notch root radius of ρ=1 mm.

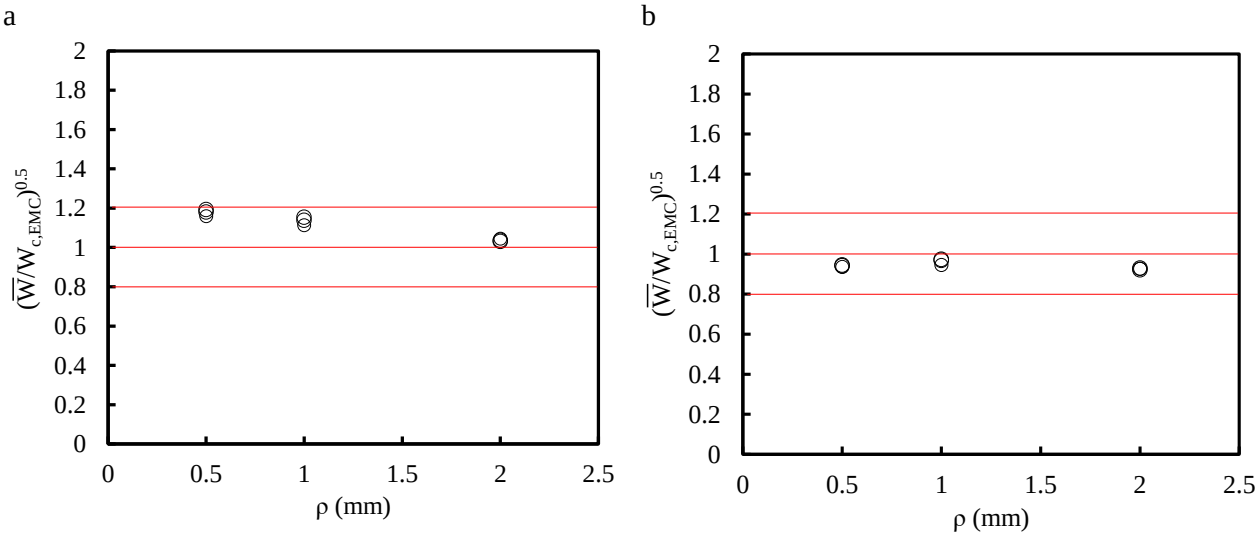

Fig. 6. Synthesis of fracture data in terms of normalized ASED; (a) Al 7075-T6, (b) Al 6061-T6.